

Cloud model of the mean quasar spectrum

Bożena Czerny¹, Anne-Marie Dumont²

¹Copernicus Astronomical Center, Bartycka 18. PL-00-716 Warsaw, Poland

²DAEC, Observatoire de Paris, Section de Meudon, 92195 Meudon, France

Received 15 December 1997; accepted 15 June 1998

Abstract. We assume a distribution of clouds optically thick for electron scattering (OTCM) which are moderately optically thin for absorption and we consider them as a model of the mean quasar spectrum of Laor et al. (1997). We show that the model is particularly sensitive to the value of the ionization parameter ξ and that for $\xi \sim 500$ the model well reproduces the optical/UV/X-ray mean quasar spectrum, in agreement with the estimates of the ionization parameter based on the energy of the iron K_α line. We cannot definitively reject synchrotron emission as a source of primary radiation but we favor the model in which the hard X-ray emission is produced by Compton scattering of soft photons in a central hot medium surrounded by cool clouds. In such a model clouds are located typically at the distance of $\sim 12R_{Schw}$, with the covering factor about 0.88 and the radius of hot plasma is $\sim 9R_{Schw}$. The model explains optical/UV emission as predominantly due to the dark sides of the clouds and the soft X-ray emission as due to the reflection by the irradiated sides of the clouds. Therefore, atomic features are expected in these bands although they are hardly present in the observational data. The kinematical effects connected with the cloud motion affect those features but do not remove them. The level of the primary emission required to model the mean quasar spectrum is too low to reproduce the equivalent width of the iron K_α line correctly but more detailed computations may resolve this problem.

Key words: galaxies:active - :nuclei - radiation mechanisms:thermal - ultraviolet:galaxies - X-rays:galaxies

A hot optically thin phase is responsible for the X-ray and γ -ray emission while a cool phase of considerable optical depth is responsible for the thermal optical/UV emission as well as for the preprocessing of a significant fraction of the radiation produced by the hot phase (for a review, see e.g. Mushotzky et al. 1993). There is mounting evidence based on the shape of $K\alpha$ line profile as well as on the variability in soft and hard X-rays, that the release of the major part of the X-ray energy, of the thermal EUV/soft X-ray emission and the reprocessing of X-ray by cold material takes place in a very compact region, of order of ~ 10 Schwarzschild radii and the cold matter is approximately in Keplerian motion (see e.g. Nandra et al. 1997a).

However, the geometrical arrangement of the two phases is still under debate. The three most viable models are: a disk with a hot corona, very optically thick clouds embedded in a hot medium, and moderately optically thick clouds also coexisting with a hot medium. In order to differentiate between these models detailed studies of all of them are necessary. The disk model is the best studied so far (e.g. Ross & Fabian 1993, Stern et al. 1995, Sincell & Krolik 1997). Optically thick clouds were studied for example by Sivron & Tsuruta (1993; see also the references therein). Clouds of moderate optical depth were broadly advertised as a 'free-free' emission model (e.g. Antonucci & Barvainis 1988). However, clouds which are optically thin for electron scattering are not a viable model for an AGN (Barvainis 1993, Collin-Souffrin et al. 1996, Kuncic et al. 1997; see also Lightman & White 1988). On the other hand clouds, which are optically thick for electron scattering but optically thin for absorption in the UV and moderately optically thick in the optical band (hereafter OTCM model), can reproduce the required fraction of the X-ray emission and roughly produce the correct multi-wavelength spectra, as well as provide enough material to support the nuclear activity (Collin-Souffrin et al. 1996; hereafter Paper I). As the model may have an advantage over clouds optically thick for absorption it deserves a detailed study of its observational consequences.

1. Introduction

It is broadly accepted now that active galactic nuclei are powered by accretion onto a supermassive black hole and that the flow is a multi-phase (at least two-phase) medium.

Send offprint requests to: A.-M. Dumont

In this paper we concentrate on the comparison of the predictions of the OTCM with the broad band mean spectrum for radio quiet quasars determined by Laor et al. (1997). As direct analysis of the X-ray emission does not give any reliable answer to the question of the nature of the X-ray and γ -ray emission due to the still poor determination of the spectra of radio quiet AGN in the $\sim 1\text{MeV}$ range (see e.g. Gondek et al. 1997 for combined Seyfert 1 spectra from GRO) we analyze three representative cases of the sources of emission external to the clouds. As is customary and convenient, we call this incident radiation for the clouds the “primary” radiation although this is unjustified when the X-ray emission is itself the emission of the clouds comptonized by a hot medium.

2. The model

The overall outline of the cloud model and of the radiation transfer within a cloud was presented in Paper I so we only summarize here the basic assumptions.

We consider a distribution of clouds surrounding a hot plasma which is a source of incident (primary) radiation for the clouds. Sides of the clouds exposed to the central source are bright while the unexposed sides are relatively dark and cold because of the considerable optical depth of the clouds. The schematic geometry is shown in Figs. 1 and 2.

All clouds are assumed to have the same density and to be exposed to the same incident flux since any assumption about the radial distribution of the cloud properties would be completely arbitrary without an underlying dynamical model. However, we carefully calculate the radiative transfer in the clouds. The resulting broad band spectra from the IR to X-rays are combinations of the radiation transmitted, emitted and scattered by clouds as well as a fraction of the primary radiation. The relative weight of these components depends on the covering factor and the size of the source of primary emission.

The radiation transfer code used in this paper (Dumont & Collin-Souffrin, in preparation) has been improved in comparison with the one used in Paper I. The ionization of all hydrogenic ions (not only hydrogen itself) proceeds from all 5 levels and interlocking (subordinate) lines are included. These modifications influence to some extent the line emission and the Lyman edge, particularly due to its coincidence with the second level of He^+ .

Since the radiative transfer code of Dumont & Collin-Souffrin is constrained in the present version to photons with energy below 24 keV (although Compton heating by harder X-rays is included) we calculate the shape of the reflected spectrum above 24 keV using the method given by Lightman & White (1988). We use the opacities for the neutral gas since the ionization level is unimportant for these high energy photons. The continuity between the two reflected spectra was achieved by adjusting the opacity parameter C of Lightman & White (1988) in their

Eq. (17). The value of this parameter was in all cases about 0.5×10^{-5} , by a factor of two lower than the value suggested by George (private communication) for a neutral medium and elemental abundances used in George & Fabian (1991).

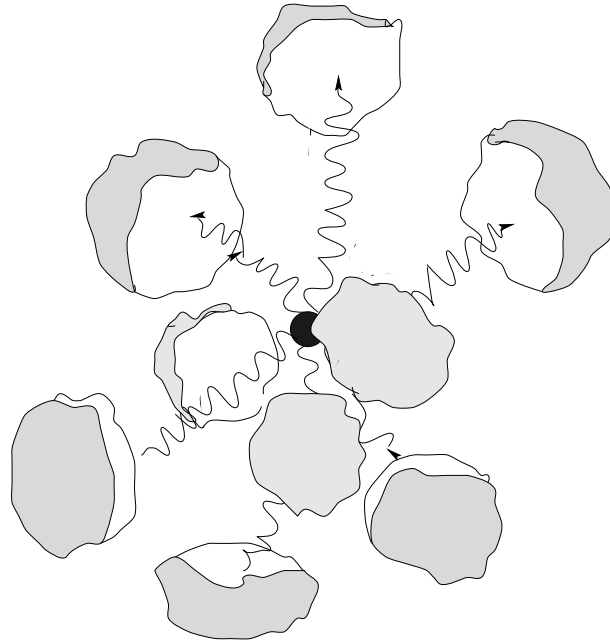


Fig. 1. The overall view of the geometry of the model (A) and (B). Clouds surround a central source of unspecified origin, with one of the clouds just accidentally partially blocking our direct line of sight to the source of primary emission.

2.1. Cloud parameters

Since, at this stage, we do not introduce a full dynamical model describing the cloud formation and disruption and their motion the radial distribution of the clouds themselves and of their properties is arbitrary. Therefore, in order to keep the parameterization as simple as possible we assume that all clouds have the same (constant throughout a cloud) density n and column density N_H . Since clouds optically thin for electron scattering were ruled out as a model for optical/UV/soft X-ray continuum we study clouds with $\log(N_H) \geq 25$, usually concentrating on the $\log(N_H) = 26$ case. Higher N_H strongly suppress the emission from the unilluminated side of the cloud so only reflection is seen. The clouds are opaque for the X-ray radiation so even if some clouds are in our line of sight towards the primary X-ray source this would not lead to the presence of the transmitted, strongly absorbed spectral component. The primary emission intercepted by the clouds is partially reflected and partially reemitted by the

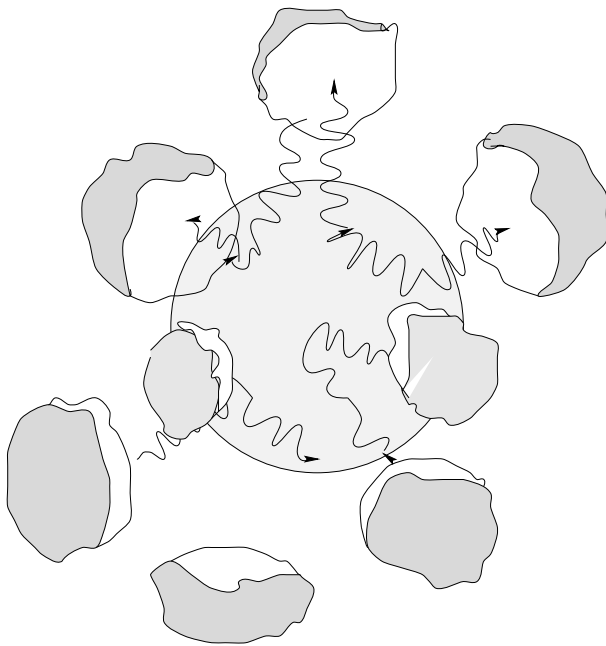


Fig. 2. The overall view of the geometry of the the model (C). Hot plasma in the center acts as a source of 'primary emission' by Compton scattering soft photons emitted or reflected by the clouds.

dark side of the cloud (i.e. the side opposite to the central source) in the form of thermal emission.

The distribution of the clouds is described by the covering factor $\Omega/4\pi$ with respect to the X-ray source. If $\Omega/4\pi$ is close to 1, the distribution necessarily is almost spherical. If $\Omega/4\pi$ is smaller (e.g. 0.5) then the distribution may either be still spherical, or rather constrained to the symmetry plane. These two cases are different if Doppler effects connected with the motion of the clouds are taken into account since plane confinement would result in broader features for the same velocity field.

2.2. The primary radiation

The nature of the primary emission is still not known. In the past, non-thermal models were favored. In such models a (usually power law) distribution of relativistic electrons produces the radiation either by direct synchrotron emission or by Comptonization of soft photons. These soft photons were either their own synchrotron photons (SSC) or came from external source like an accretion disk. In these models the pair creation process was frequently important, particularly for the shape of the spectrum above $\sim 1\text{MeV}$.

These models are still very popular in the case of radio loud AGN. However, in the studies of radio quiet AGN the attention recently shifted towards thermal models. In these models the hot plasma is thermal, at a temperature

of order of a few hundreds of keV, and it produces the radiation through Comptonization of soft external photons. In these models the effect of pair creation is usually negligible.

These two basic families of models differ also in the extension of the primary component into the low energy range. In non-thermal models the primary emission may (but does not necessarily have to) extend down to the far-IR/mm band. It was an attractive possibility in the late 70s and 80s when IR emission was generally thought to be dominated by non-thermal processes. Evidence of a significant contribution of dust to the IR emission as well as some arguments based on variability (e.g. Done et al. 1990 for NGC 4051) diminished the popularity of that view. However, a single underlying IR/X-ray continuum is still sometimes advocated on the basis of observational arguments (e.g. Walter & Fink 1993, Loska & Czerny 1990, Fiore et al. 1995). Thermal models, on the other hand, predict a contribution of the hard component only above the energy of the seed photons for Comptonization, i.e. mostly starting from the UV band.

As a result, in their computations of the overall continua, various authors used different specific assumptions about the shapes of the incident spectra for reprocessing. Lightman & White (1988) consider a non-thermal model with an energy index 0.7 and a spectrum extending from 1 eV to 3 MeV, Guilbert & Rees (1988) have the primary non-thermal spectrum with energy index 0.5 (they also include the effect of pair creation on the shape of the primary). Sivron & Tsuruta (1993) assume that the initial synchrotron radiation with an energy index 1 extending from 0.1 eV to 1 MeV is filtered by CFR cloudlets (Celotti et al. 1992). This special, very compact, population of cloudlets, with densities $\sim 10^{16-18}\text{cm}^{-3}$, hydrogen column $N_H \sim 10^{21}\text{cm}^2$ and covering factor 1, absorbs the IR emission (through the free-free process) but it is transparent at the optical band and above. The absorbed energy is reemitted in the form of free-free emission with the adopted value of the temperature 10^6 K. Such a preprocessed spectrum serves as incident spectrum for the main clouds occupying the space between $R_{in} = 10R_{Schw}$ and $R_{out} = 1000R_{Schw}$.

In order to study the influence of the shape of the incident flux on the resulting spectrum predicted by the model we choose three representative shapes of the primary continuum justified by general theoretical arguments. They are named models (A), (B) and (C), and they are shown in Fig. 3.

2.2.1. Model A: synchrotron emission extending to IR

This incident radiation resembles closely the incident radiation adopted in our initial study (Paper I) as well as by Kuncic et al. (1997). We assumed a low frequency cut-off at 0.1eV as in Paper I. In order to reproduce well the observed spectrum (according the present knowledge) we

assume an energy index either 0.9, after the classical paper on Seyfert 1 galaxies (Pounds et al. 1990) or steeper since in the case of quasars the situation is not clear: Laor et al. (1997) give a slope of 1 for radio quiet objects while Williams et al. (1992) give 0.92 when flat spectrum objects are excluded. We assume the values of the cutoff energy 100 keV and 280 keV since this last value seems to be suggested by GRO data for Seyfert 1 galaxies (Grandi et al. 1998 for MCG8-11-11; Madejski et al. 1995 for IC 44329A, Gondek et al. 1997 for a composite spectrum). No direct data constraints for cut-off energy in radio quiet quasars are available.

Such a model corresponds to the presence of a relatively strong magnetic field within the hot plasma, such that the energy density of the magnetic field is larger than the energy density of the soft photons available due to the presence of cool clouds. Models of that type were studied e.g. by Maraschi et al. (1982), with lower frequency cut-off $10^{12} - 10^{13}$ Hz determined by self-absorption.

The hypothesis of the existence of such an IR/X-ray power law was observationally tested in the case of the source NGC 4051 (Done et al. 1990) and its existence was not confirmed since strong X-ray variability in this source was not accompanied by any optical variability. On the other hand NGC 4051 is not a typical example of an AGN and its optical emission may be strongly dominated by starlight. A number of other sources like NGC 5548 (Korista et al. 1995) and NGC 4151 (Edelson et al. 1997) show coherent day to day variations in optical, UV and X-ray band, with unmeasurable delays smaller than several hours.

We do not analyze the conditions for the production of such a primary emission in the present paper. We simply assume the parametrization by a single power law and we fix the low energy cut-off at 0.1 eV, as in Paper I.

The input model parameters are: the ionization parameter, $\xi = L/nR^2$ (where L is the bolometric luminosity), the cloud density, n , and its hydrogen density column, N_H , (or cloud size). The observational appearance of the system is further parameterized by the relative contribution of the primary (or incident) radiation and the emission from dark sides of clouds with respect to the reflected component. For purely random cloud distribution both parameters are uniquely determined by the covering factor, $\Omega/4\pi$ (see eq. 2).

2.2.2. Model B: synchrotron emission extending to UV

Our second model is a power law characterized by the same energy index and high energy cut-off as before but the adopted low frequency cut-off is set at 30 eV i.e. in the UV band (7×10^{15} Hz). This simple model is supposed to represent a situation when the gas is not simply in equipartition with the magnetic field but dominates the behaviour of the matter (Rees 1987). As the expected magnetic field is in this case two orders of magnitude or more higher than

in the previous case ($B \sim 10^4 - 10^5$ gauss, see Celotti et al. 1992) the self-absorption frequency is proportionally higher. Additionally, in such a strong magnetic field a new family of cloudlets, or filaments, may form in the innermost part of the flow. Such cloudlets are opaque to photons below, again, 10^{15} Hz due to their high density and free-free absorption so they filter the primary emission before this emission may reach the main clouds outside (Sivron & Tsuruta 1993). Therefore the incident radiation in the case of magnetic field dominating innermost flow would not extend beyond optical/UV. Absorption by cloudlets leads additionally to reemission of the absorbed radiation in the form of a black body radiation. However, as we cannot predict the temperature of such radiation and the covering factor by the inner cloudlets we simply neglect this component in the present consideration.

The input model parameters are the same as in the previous section.

2.2.3. Model C: self-consistent thermal model

This model is based on the assumption that amplification of the magnetic field within the flow is not efficient. Therefore, clouds are the only source of the soft photons. We also assume this time that the hot medium is thermal, i.e. basically characterized by the optical depth and the temperature. Hard X-ray emission in this model forms by Compton upscatter of a fraction of the soft photons from the clouds while soft photons result from interception of a fraction of hard X-ray emission by clouds.

In order to obtain the appropriate shape of the hard X-ray continuum as described above we have to adopt a temperature of the hot medium equal to $\sim 3 \times 10^9$ K and an optical depth ~ 0.1 . Adopting higher (lower) value for the temperature would require a lower (higher) value of the optical depth of the hot medium. The Compton parameter y for such a plasma is 1.1.

The fraction of the soft photons intercepted by the hot medium results from the model (see Paper I) and is approximately given by

$$\left(\frac{R_X}{R_{UV}}\right)^2 = \frac{4\pi}{\Omega f_X \exp(y)} \quad (1)$$

where f_X is the fraction of photons reflected or reemitted by the illuminated side of a cloud, determined by the physical conditions in the gas. Our model is therefore more flexible than the original version of the corona model (Haardt & Maraschi 1991) which requires $\Omega/4\pi$ equal to 0.5 and $R_X = R_{UV}$, thus practically fixing the value of the Compton parameter y . Recently developed clumpy corona models are based on an additional covering factor for the hot medium which is equivalent to our R_X/R_{UV} ratio from the point of view of the efficiency of the Comptonization but the two models nevertheless differ with respect to overall geometry and its (angular-dependent) appearance.

The input parameters of the model are, as usual, the ionization parameter, the cloud density, its hydrogen density column (or size), and the weights of the primary and dark side components.

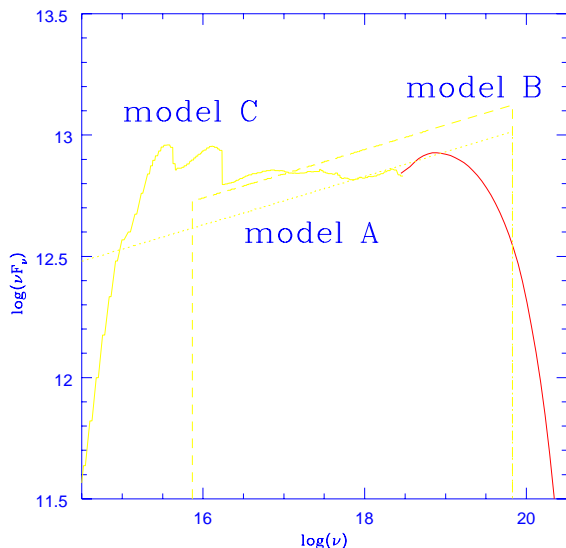


Fig. 3. Three examples of the IR-X-ray incident (primary) spectra for OTCM models, as described in Section 2.2: model (A) - dotted line, model (B) - dashed line and model (C) - continuous line. Model C was computed assuming the hot medium temperature equal to 3×10^9 K and its optical depth equal to 0.1.

However, the computations of the model require an iterative procedure to achieve a self-consistent solution for the soft and hard emission. In order to avoid an arbitrarily adopted spectral shape in the optical band we start with a mechanically heated cloud with temperature $\sim 10^5$ K. Next we compute the Comptonized spectrum which results from the interception of soft photons by hot plasma with the parameters given above. For that purpose we use the method of Czerny & Zbyszewska (1991), appropriate for a thin plasma. This radiation now serves as incident radiation. Next we calculate the **reflected** (not emitted) component as the cloud faces the hot medium clearly with its hot hemisphere. The comptonization of this reflected component gives a second approximation to the hard X-ray emission spectrum and the model is iterated until it converges. The normalization is fixed by the adopted value of the ionization parameter and the ratio of the Comptonized reflected radiation to renormalized radiation gives us accurately the fraction of soft photons intercepted by the hot gas, or the relative extension of the two regions, roughly estimated by Eq. (1).

3. Results

The observed spectrum of an AGN within the frame of the OTCM is in general a sum of the primary, a reflected component and an emission from the dark sides of the clouds, with the relative weight of the last two given by the covering factor (see Paper I). We make first a general qualitative discussion without adopting any specific value of this parameter (Sect. 3.1). More detailed discussion, however, clearly involves the covering factor as additional parameter of the model (Sect. 3.2 and 3.3).

3.1. General properties of the primary, reflected and emitted components

3.1.1. The choice of the cloud parameters

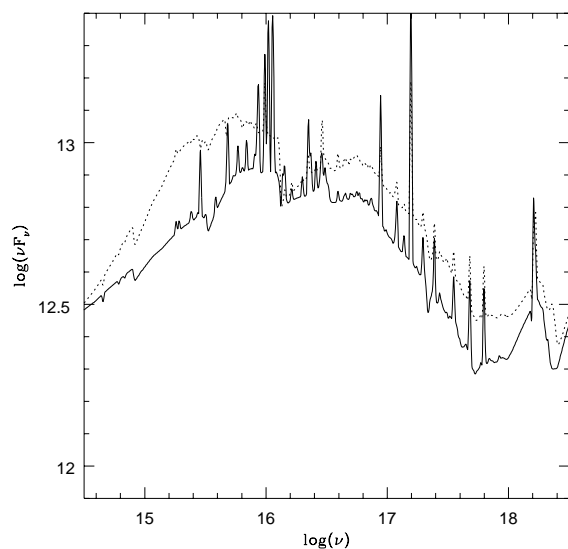


Fig. 4. Two examples of the optical/X-ray spectrum coming from the bright sides of clouds calculated for model (A) assuming the cloud column density 10^{25} cm^{-2} (continuous line) and 10^{26} cm^{-2} (dotted line). Other parameters: ionization parameter $\xi = 1000$, extension of the incident spectrum from 0.1 eV to 280 keV, the slope of the incident spectrum $\alpha = 0.9$ and cloud density 10^{12} cm^{-3} .

The clouds are parameterized by the density, n , and the hydrogen density column, N_H . The reflected radiation, i.e. the radiation of the bright illuminated sides of the clouds is not very sensitive to the column density as long as the total optical depth of a cloud is high and in this paper we deal with such a clouds. In Fig. 4 we show two examples of the reflected spectra for two values of the column density (for model A). We see that the spectrum is softer in the optical band and slightly harder in the soft X-rays. The column density is important, however, for determination

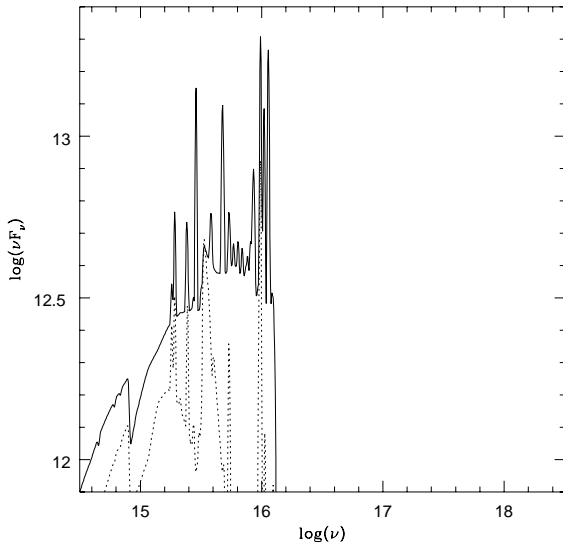


Fig. 5. Two examples of the optical/X-ray spectrum coming from the dark sides of clouds calculated for model (A) assuming the cloud column density 10^{25} cm^{-2} (continuous line) and 10^{26} cm^{-2} (dotted line). Other parameters: ionization parameter $\xi = 1000$, extension of the incident spectrum from 0.1 eV to 280 keV, the slope of the incident spectrum $\alpha = 0.9$ and cloud density 10^{12} cm^{-3} .

of the emission of the dark sides of the clouds (see Fig. 5). Larger column density leads to almost a black body type of emission although atomic features are clearly visible while lower column density is characterized by very strong atomic features superimposed on the continuum. The comparison with optically thin clouds was already discussed in Paper I.

Examples of the spectra calculated for three values of the ionization parameter ξ (300, 1000 and 3000) were shown in Paper I.

The dependence on the density of the clouds is weak since we parameterize the incident radiation not by flux but by the ionization parameter ξ . Clouds with lower density (10^{10} cm^{-3}) are characterized by slightly bigger hydrogen and helium edges. Clouds with larger densities (10^{14} cm^{-3}) are slightly optically thicker in the optical range thus leading to lower emission in those wavelengths.

3.1.2. The high energy extension and the slope of the primary emission

We tested two values of the high energy extension of the incident spectrum: 100 keV and 280 keV. The effective change of the bolometric luminosity required to preserve the value of the ionization parameter is practically negligible. However, high energy photons penetrate more easily deeper layers of the clouds so the radiation is thermalized

more effectively and the UV part of the reflected spectrum as well as the dark sides of clouds are slightly brighter.

More important role for the shape of the reflected spectrum is played by the slope of the incident radiation. In Fig. 6 we show two examples of model A (reflected spectrum) calculated for the energy index α equal to 0.9 and 1.1. Steeper spectrum of the incident radiation results in steeper (i.e. softer) spectrum both in the optical band and in the soft X-rays.

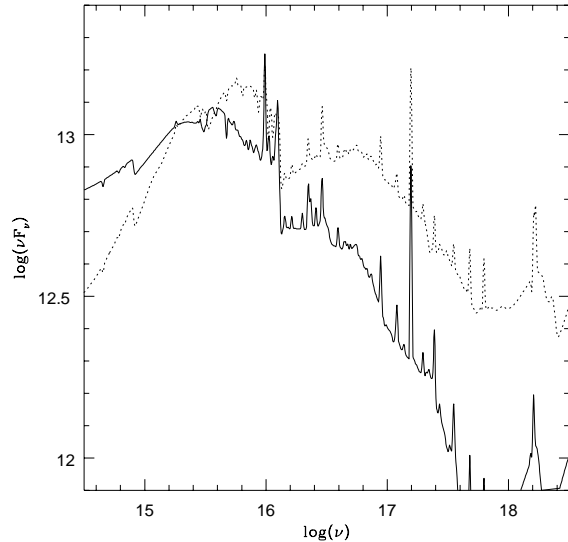


Fig. 6. Two examples of the optical/X-ray spectrum coming from the bright sides of clouds calculated for model (A) assuming the slope $\alpha = 0.9$ (dotted line) and 1.1 (continuous line). Other parameters: ionization parameter $\xi = 1000$, extension of the incident spectrum from 0.1 eV to 280 keV, cloud density 10^{12} cm^{-3} and the column density 10^{26} cm^{-2} .

3.1.3. The nature of the primary emission

In order to show the dependence of the OTCM model on the assumption about the primary emission we present examples of solutions in which identical distributions of clouds are exposed to primary emission with the same ionization parameter but different spectral properties. The shapes of the incident spectra were shown in Fig. 3.

In the IR/optical band model (A) is different from the other two. If the covering factor of the source is not close to 1 the primary emission directly contributes to this spectral band and may strongly modify the optical slope of the resulting spectrum (see also Section 3.2) making it softer. The visibility of the primary emission in that energy band also affects the variability since in this case a fraction of the optical emission is not expected to be delayed with respect to the X-ray band.

In the EUV/X-ray band model (C) is significantly different from the other two models. Power law models are featureless while the Comptonization of the radiation emitted by the clouds preserves traces of atomic features if the optical depth of the hot medium is lower than ~ 0.5 . Therefore in synchrotron models all line emission (in particular, Fe K_α line) has to be delayed with respect to the power law while in the last case the clear division of the X-ray emission into primary and reflected component is difficult and a fraction of the line flux does not have to be delayed with respect to power law.

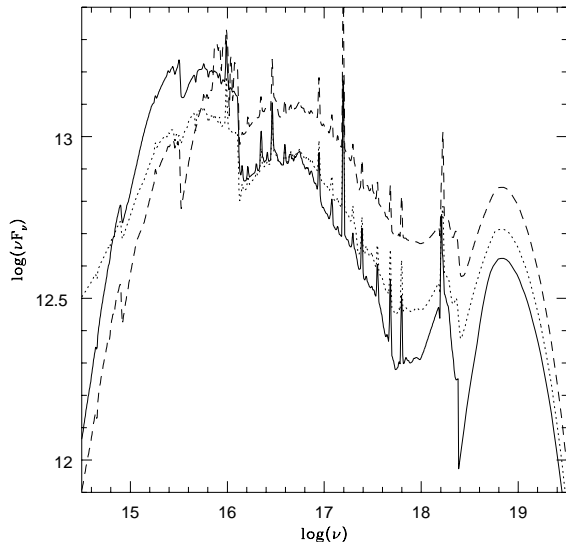


Fig. 7. Three examples of the IR-Xray spectrum reflected from OTCM clouds calculated under assumptions of three primary emission models described in Section 2.2: model (A) - dotted line, model (B) - dashed line, model (C) - continuous line. In all cases the ionization parameter of the clouds is equal to 1000, cloud density is 10^{12} cm^{-3} and the column density is 10^{26} cm^{-2} .

The extension of the primary emission into gamma band simply reflects the adopted assumptions.

The spectra reflected by the clouds are shown in Fig.7. The emission lines are included; they are plotted adopting a spectral resolution $\nu/\delta\nu$ equal to 30. The properties of the three spectra are influenced by the choice of the primary emission mechanism.

The model (A) presented here differs with respect to the model given in Fig. 9a of Paper I mostly because of the change in the shape of the incident radiation (slope of 0.9 instead of 1.0, and the high energy cutoff (280 keV instead of 100 keV). The new spectrum is generally harder because the incident radiation is harder and elastically scattered photons constitute a significant fraction of the reflected spectrum. The improvement of the physical input

into the code resulted in slightly stronger emission lines and a more shallow Lyman edge.

The optical/UV slope of the reflected component is significantly flatter in the case of model (A) than in the other two. However, the traces of a Balmer edge and of a significant Lyman edge can be seen in all these spectra.

The soft X-ray part of the reflected spectrum looks similar in all three models as it is mostly determined by the adopted value of the ionization parameter. There is considerable emission below 2 keV with an approximate photon index 2.5 between 0.2 and 2 keV. The strong Fe K_α line is also characteristic for all three spectra, but the K_α edge is the weakest for model (A) and the most profound for model (C).

The broad band spectral index α_{ox} , measured customary between 2500 Å and 2 keV, for the reflected component itself is equal to 1.09 for model (A), 0.94 for model (B) and 1.14 for model (C).

The high frequency part of the spectrum is again similar in all three cases which is due to the fact that the shape of the reflection component at high frequencies is simply determined by the Klein-Nishina cross-section for scattering.

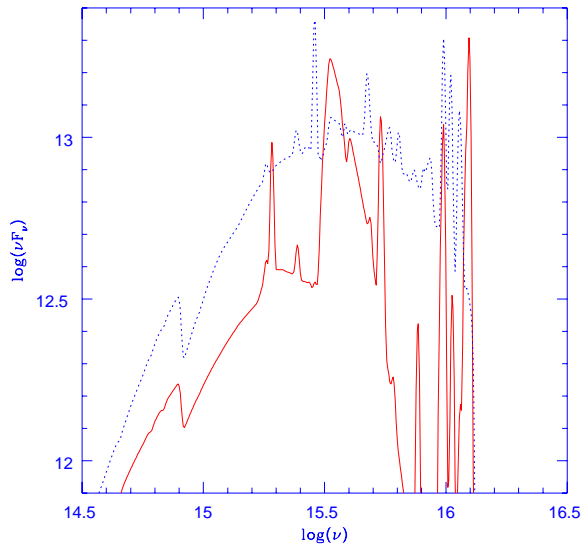


Fig. 8. The emission of the dark sides of OTCM clouds calculated under assumptions of model (C) described in Section 2.2.1 (continuous line). Dotted line shows a case (A) spectrum but with the temperature of the dark side of the cloud equal to $5 \times 10^4 \text{ K}$, higher than results from pure radiative heating. The ionization parameter of the clouds is equal to 1000, cloud density is 10^{12} cm^{-3} and the column density is 10^{26} cm^{-2} .

An example of radiation spectra emitted by the dark sides of the clouds is shown in Fig. 8. The figure shows case (C) but the other two spectra are also characterized

by an extremely large Lyman discontinuity in emission unless an extra heating of the dark sides of the clouds is allowed (dotted line).

For these spectra the α_{ox} index is high in all cases since the contribution of the dark side of the clouds to the spectrum at 2 keV is negligible. Therefore any contribution of the dark sides of the clouds to the resulting spectra would give steeper α_{ox} than pure reflection spectra. Any contribution from primary emission would work in the opposite direction, and additionally it would modify the soft X-ray slope.

3.2. Optical/UV slope

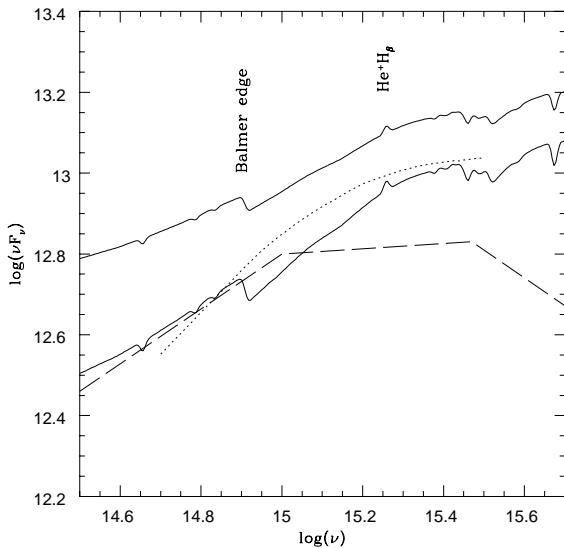


Fig. 9. Optical/UV spectrum of OTCM clouds calculated under assumptions of emission model (A) described in Section 2.2.1. The lower curve shows the reflected spectrum and the upper curve shows a case of an equal contribution from the reflected and primary emission. The ionization parameter of the clouds is equal to 1000, cloud density is 10^{12} cm^{-3} and the column density is 10^{26} cm^{-2} . The dashed line shows the mean spectrum of radio quiet quasars from Laor et al. (1997) and the dotted line shows the mean quasar spectrum of Francis et al. (1991).

We show an expanded fragment of the spectrum calculated from model (A) in Fig. 9. We consider two extreme cases interesting from the observational point of view. The lower curve shows a pure reflection component, i.e. corresponds to the case when the primary emission is not seen directly because it comes from a compact source and is shadowed by one of the clouds. The upper curve was obtained assuming that half of the primary source emission reaches the observer.

In both cases we see the characteristic atomic features: noticeable Balmer edge, Lyman edge and weak He^+H_β line. Equally profound spectral features are seen in models (B) and (C) since the spectral shape of the incident radiation has little effect. The Comptonization within the clouds is not expected to remove these features for the clouds of the adopted properties and $\xi = 1000$ (Paper I).

The clear difference between model (A) and models (B) and (C) is in the slope of this part of the spectrum. We compare the models with the mean spectrum for radio quiet quasars derived recently by Laor et al. (1997). Our case (A) nicely coincides with the data in the optical part (if primary and the dark sides of the clouds are not seen) but is far too bright in the UV which means that the temperature of the clouds is too high. In the case of model (B) and (C) the reflection spectra are definitely too hard in the optical band and any contribution from the primary emission does not change that.

The comparison with the mean quasar spectrum obtained by Francis et al. (1991) is more favorable for model (A) and in that case a minor contribution from the primary emission would even be allowed. However, models (B) and (C) are still too hard to match observations for the ionization parameter $\xi = 1000$.

Any contribution from the emitted spectra would give still harder spectra, in contradiction with the data.

The choice of lower value of the ionization parameter ξ results in a lower value for the cloud temperature which in principle helps to reconcile the models (B) and (C) with the data. We computed the spectra assuming $\xi = 300$. However, in that case the spectral features (Balmer edge in absorption and Lyman edge in emission) are strong, giving a change in the continuum by 50 % and 100 %, respectively, in the case of a reflection component and even more (100 % and 500 % respectively) in the case of emission from the dark sides of the clouds.

3.3. Soft X-ray emission

Since the spectrum emitted by the dark sides does not contribute to the soft X-rays we can restrict our study of that band to the reflected component and the contribution from the primary emission.

We show an expanded version of model (A) in Fig. 10, in two versions: pure reflection spectrum and reflection plus two half of the primary emission. We assumed $\xi = 1000$.

The overall shape of the spectrum looks like a power law. When pure reflection is considered the slope of this power law is similar to the mean spectrum of radio quiet quasars (Laor et al. 1997). If a significant contribution from the primary is allowed the slope is too flat. Models (B) and (C) are generally similar in this spectral band so they are also an adequate description of the data.

Precise values of the slope between 0.2 keV and 2 keV for the reflected component in the three models are equal to 1.48, 1.35 and 1.57, respectively. The slope in the Laor

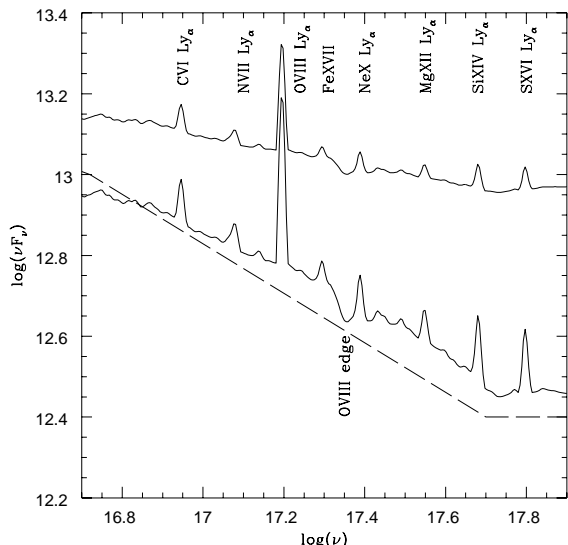


Fig. 10. Soft X-ray spectrum of OTCM clouds calculated under assumptions of emission model (A) described in Section 2.2.1. The lower curve shows the reflected spectrum and the upper curve shows the observed spectrum for the weight from primary 0.5. The ionization parameter of the clouds is equal to 1000, cloud density is 10^{12} cm^{-3} and the column density is 10^{26} cm^{-2} . The dashed line shows the mean spectrum of radio quiet quasars from Laor et al. (1997).

et al. (1997) sample is 1.6 so model (C) is the best representation of the data. Even in the last model there is no place for a significant contribution from the direct primary emission since the slope would be too flat.

We see a number of quite strong emission lines, with OVIII at 0.653 keV being the most prominent. Complex spectral features are observed in a number of sources both in absorption and in emission, and they are usually explained by warm absorbers, i.e. optically thin clouds with a column density $\sim 10^{23}$ and located at a distance of several light weeks (e.g. Otani et al. 1996). The same features are seen in models (B) and (C). Neither the mean quasar spectrum of Laor et al. (1997) nor observations of single quasars (e.g. Leach et al. 1995 for 3C 273) indicate the presence of such features.

A higher value of the ionization parameter would give too flat slopes for all three models.

Lower values of the ionization parameter give systematically steeper slopes. Model (A) calculated for $\xi = 300$ requires a contribution of the primary emission with a weight of 0.2 in order to reproduce the observed slope. For model (C) the allowed contribution of the primary is always slightly higher for a given value of the ionization parameter, and for $\xi = 500$ the required weight of the primary is ~ 0.15 . The line emission is much stronger in that case.

In any case, the OTCM model for quasars explains the soft X-ray emission as a reflection from a partially ionized gas. The same mechanism was suggested to produce weak soft X-ray excesses in a number of Seyfert 1 galaxies (Czerny & Życki 1994). However, in their case there were some problems to achieve the required ionization state of the gas within the frame of the adopted model. No such problems are encountered here.

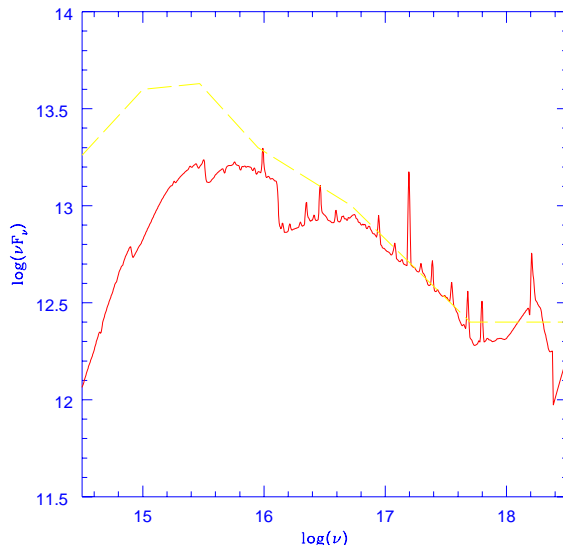


Fig. 11. Optical/UV/soft X-ray spectrum of OTCM clouds for pure reflection calculated under assumptions of emission model (C) described in Section 2.2.1 (continuous line). The ionization parameter of the clouds is equal to 1000, cloud density is 10^{12} cm^{-3} and the column density is 10^{26} cm^{-2} . The dashed line shows the mean spectrum of radio quiet quasars from Laor et al. (1997).

3.4. Matching soft X-ray emission with UV

So far we discussed the comparison of the models with the mean quasar spectrum in the optical/UV band and in the soft X-ray band separately, i.e. with an arbitrary normalization in both bands. The comparison of the data with the model in the entire optical/UV/soft X-ray band is shown in Fig. 11 (model C, pure reflection). If the normalization is adjusted to soft X-rays we notice that the observed flattening towards high X-rays (at $\sim 2 \text{ keV}$) is reproduced by the models.

The α_{ox} index of the mean quasar spectrum of Laor et al. (1997) is equal to 1.46 while in the reflected spectra shown in Fig. 7 it is equal to 1.09, 0.94 and 1.14, respectively. However, a contribution of the emission of the dark sides of the clouds helps to fill the gap.

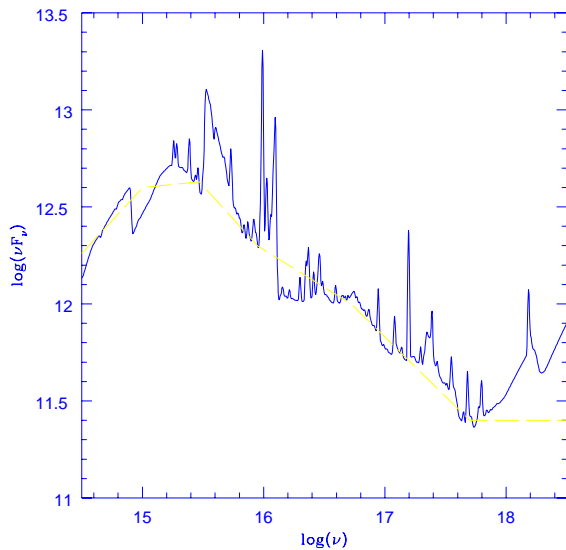


Fig. 12. Optical/UV/soft X-ray spectrum of OTCM clouds calculated under assumptions of emission model (A) described in Section 2.2.1 (continuous line) and assuming the weight of the reflected radiation equal to 1.0, of the dark sides emission 1.2, and of the primary 0.15. The ionization parameter of the clouds is equal to 300, cloud density is 10^{12} cm^{-3} and the column density is 10^{26} cm^{-2} . The dashed line shows the mean spectrum of radio quiet quasars from Laor et al. (1997).

Since the temperature of the dark side of a cloud depends significantly on the value of the ionization parameter ξ we can adjust its value to model the UV/EUV spectrum (apart from the spectral features present in the model and absent in the data).

In the case of model (A) the best value of the ionization parameter is ~ 300 and an example of the resulting spectrum is shown in Fig. 12. Even the slight bend below $\sim 0.2 \text{ keV}$ is reproduced by the models. The contribution of the dark sides of the clouds required to provide the flux in the optical band is rather moderate and the entire spectrum is mostly dominated by reflection. In the case of model (C) the best value of the ionization parameter is slightly higher, ~ 500 (see Fig. 13). However, there is a large deficit of emission in the optical band which shows that a number of additional, cooler clouds should be included in the model, i.e. a single cloud population located at a given distance (i.e. parametrized by a single value of ionization parameter) is not an adequate description of the data in the case model (C).

The spectral features in the optical/UV band are quite large in that case. The kinematic broadening of these features due to the motion of the clouds may slightly reduce and broaden those features (see Fig. 15 for this effect in the soft X-ray band) but will not really remove them and we intend to devote a special paper to that problem since

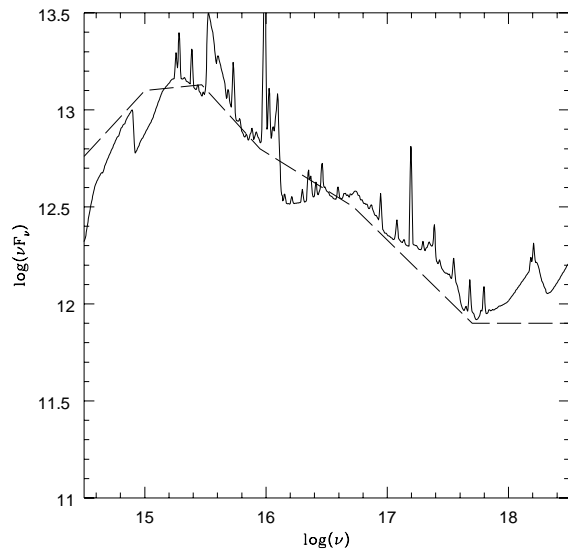


Fig. 13. Optical/UV/soft X-ray spectrum of OTCM clouds calculated under assumptions of emission model (C) described in Section 2.2.1 (continuous line) and assuming the weight of the reflected radiation equal to 1.0, of the dark sides emission 5.0, and of the primary 0.15. The ionization parameter of the clouds is equal to 500, cloud density is 10^{12} cm^{-3} and the column density is 10^{26} cm^{-2} . The dashed line shows the mean spectrum of radio quiet quasars from Laor et al. (1997).

it is one of the major issues in all realistic models, including accretion disks.

3.5. High energy tail and the level of primary emission

The high energy cut-off of the spectrum is not well constrained observationally in the case of radio quiet quasars. Therefore, it is difficult to formulate any preferences for any of the discussed models on the basis of this spectral band.

The intensity of the iron K_{α} line given by the model is clearly large, in contradiction with observations of quasars, since a significant contribution from the primary emission is not allowed. For $\xi = 1000$ the EW is $\sim 1200 \text{ eV}$ if the direct primary emission is not seen (lower curve in Fig. 14) but it is reduced to $\sim 240 \text{ eV}$ if the contribution with a weight 0.5 would be allowed (upper curve in Fig. 14). For lower ξ it is still larger, and equals $\sim 2.3 \text{ keV}$ and $\sim 460 \text{ eV}$, respectively. This is not surprising if the reflected spectrum dominates since the line intensity expected in such case is large (e.g. Życki & Czerny 1994).

Observations of moderately bright quasars (Nandra et al. 1997b) give the equivalent width of the iron K_{α} line not higher than 300 eV , with a clear trend for a decrease of this value with an increase of a quasar luminosity.

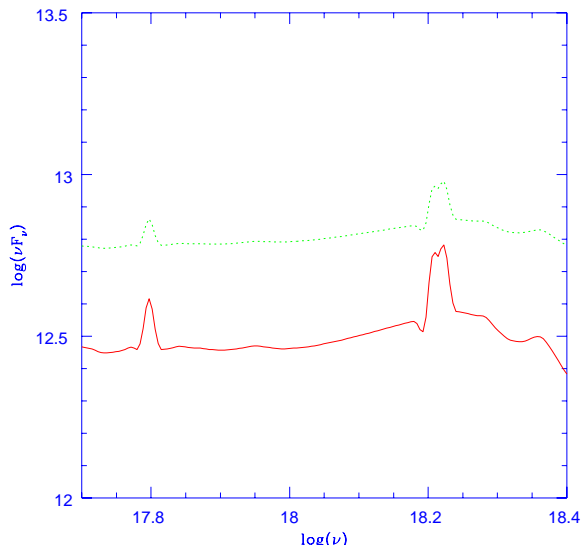


Fig. 14. The spectrum of OTCM clouds calculated under assumptions of emission model (A) described in Section 2.2.1 (continuous line). Dotted line shows a case (A) spectrum with the contribution from the primary with the weight 0.5. The ionization parameter of the clouds is equal to 1000, cloud density is 10^{12} cm^{-3} and the column density is 10^{26} cm^{-2} .

4. Discussion

4.1. Nature of primary emission

We used our OTCM model from Paper I in order to analyze the requirements which result from the comparison of the three variants of the model to Laor et al. (1997) mean spectra of radio quiet quasars. The advantage of concentrating on quasars was in a reliable description of their broad band spectra from optical band to hard X-rays.

Model (A) reproduces well the entire broad band spectrum of quasars, including the optical slope of the data. On the other hand, present computations carried for that model allow only a minor contribution from the primary emission which results in a too high equivalent width of the iron K_{α} line and a need of some special geometry for cloud distribution in order to explain this level of primary emission (see Section 4.3).

Model (B) is the least attractive since it displays the same problems as model (A) with respect to the level of primary emission and it does not explain the optical slope of quasars.

Model (C) is also too steep (i.e. too hard) in the optical band in comparison with the mean quasar spectrum although it models well the UV/X-ray band. This may mean that model (C) well represents well the innermost part of the accretion flow but it has to be supplemented by the presence of more distant clouds and/or an outer accretion disk. However, this model also display the prob-

lem of too high equivalent width of the iron K_{α} line since it again allows only a marginal contribution of the direct primary emission.

4.2. Ionization level

The modelling of the overall shape of the spectrum was very sensitive to the choice of the ionization parameter ξ since this parameter determines the cloud temperature and the emission from their dark sides which dominate the optical/UV part of the spectrum.

Our analysis based on the overall spectral shape clearly favored an ξ of order of 300-500 to fit the mean quasar spectrum of Laor et al. (1997). The value $\xi = 1000$ gave a cloud temperature too high to fill the gap in the optical band between the model predictions and the observed spectra if the soft X-ray band was modelled correctly. It also left no room for any presence of the primary emission since the soft X-ray slope of the reflected component was just marginally steep enough for model (C) to match the data.

We can compare this result with more detailed spectroscopic constraints.

The most direct estimate of the ionization level of the cool gas in quasars comes from the analysis of the position of the FeK_{α} line. ASCA results show that for moderately bright quasars the line is at 6.4 - 6.5 keV, while for bright quasars it is at 6.57 keV (Nandra et al. 1997b). This suggests that the ionization parameter for bright quasars is of the order of a few hundreds (e.g. Życki & Czerny 1994). In fact, the flux averaged position of the iron line in our computations is 6.82 keV for $\xi = 1000$, model (A), 6.43 keV for $\xi = 300$, and 6.61 keV for $\xi = 500$, model (C). Therefore, also from this point of view, all intermediate value of ξ better corresponds to the observations.

4.3. Geometry of clouds distribution and the level of primary emission

In the case of purely random distribution of clouds with a covering factor $\Omega/4\pi$ and averaged observing angle the relative contribution of the primary emission should also be determined by the covering factor, thus giving a formula appropriate for modelling a mean spectrum:

$$F_{obs} = \left(1 - \frac{\Omega}{4\pi}\right)F_i + \frac{\Omega}{4\pi}F_{dark} + \frac{\Omega}{4\pi}\left(1 - \frac{\Omega}{4\pi}\right)f_{ampl}F_r \quad (2)$$

where f_{ampl} is the amplification factor taking into account the multiple scattering

$$f_{ampl} = \left(1 - \frac{A\Omega}{4\pi}\right)^{-1} \quad (3)$$

where A is the effective albedo approximately equal 0.85 (see Paper I). This formula gives the maximum efficiency since it assumes that the source of primary emission does not intercept repeatedly scattered radiation. Other quantities have the same meaning as in Paper I, i.e. F_i is

the primary (incident) radiation, F_{dark} is the emission of the dark sides of the clouds and F_r is the radiation reflected/reemitted by the bright sides of the clouds. In the case of model(C) the amplification factor is decreased by the presence of hot plasma intercepting a fraction of the photons and the appropriate formula is given by

$$f_{ampl} = (1 - A(1 - (\frac{R_X}{R_{UV}})^2)) \frac{\Omega}{4\pi}^{-1} \quad (4)$$

Such an approach reduces the number of the original free parameters of the model as all weights are now expressed by the covering factor $\Omega/4\pi$ which allows us to test the consistency of the derived model parameters with the random distribution of clouds.

In the case of model (A) and $\xi = 300$ the Laor et al. (1997) data were reproduced by the model with the relative weights of the components in Eq. (2) equal to 0.15, 1.2 and 1.0. If we rely on the relative weight of the second and third term, this result can be translated into a covering factor $\Omega/4\pi = 0.57$. The role of the amplification is taken into account ($f_{ampl} = 1.9$). Such a cloud distribution, while reproducing precisely the normalization of the last two components, predicts a significantly larger value of the primary contribution (0.90 instead of 0.15). Lower amplification still widens this gap. This means that either the cloud distribution is not random or our theoretical spectra are too hard (i.e. flat) in the soft X-ray band. Since the equivalent width of the Fe K_α line produced by the model is also too large if the primary level is as low as 0.15 it strongly suggests that the geometry is correct but the reflection spectra should be improved.

The size of the primary source could in principle be estimated from the statistical properties of the observational sample of objects. We can only infer that the source is probably not too compact in comparison with the clouds distance from the center since a point like source would give two distinct classes of objects: a fraction of objects dominated by primary emission and the rest of the sources with the primary completely hidden from an observer, which seems not to be the case.

In the case of model (C) a slightly higher value of ξ seems to be favored, of order of 500. The relative weights of the components are equal to 0.15, 5.0 and 1.0. Therefore, dark sides of the clouds are contributing more to the total spectrum. However, now the amplification is weaker by a factor $1 - (R_X/R_{UV})^2$ due to the size of the hot cloud. Combining the requirements for the relative contribution of the reflected component, dark side component and equation (1) we obtain $\Omega/4\pi = 0.88$ and $R_X/R_{UV} = 0.66$. Such a model predicts the contribution from the primary (hot plasma in that case), of order of 0.65, a factor of 4 higher than allowed by the data.

It is interesting to note that the condition for the size of the hot plasma cloud (eq. 1) leads to a reasonable value of the R_X/R_{UV} ratio for the value of the Compton pa-

rameter y which resulted from the choice of the plasma parameters giving the hard X-ray slope of index ~ 0.9 .

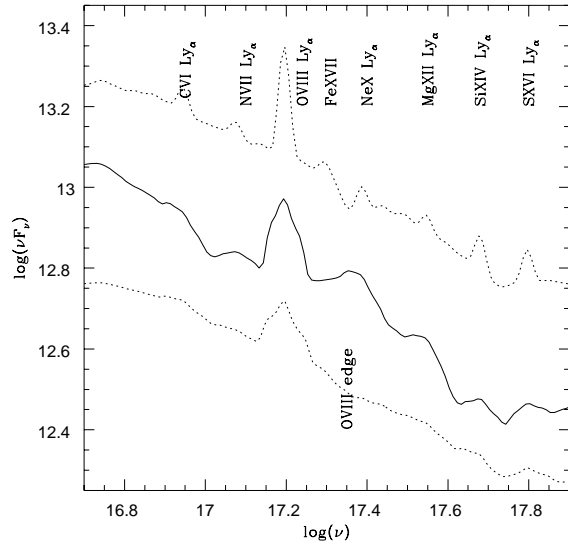


Fig. 15. The importance of the kinematics for the spectral features in the soft X-ray spectrum of OTCM clouds. The upper dotted line shows the spectrum from Fig. 10 (model A) but coming from clouds located at randomly oriented orbits of the radius $50R_{Schw}$, the lower dotted curve shows the same spectrum but from clouds circulating at $7R_{Schw}$ and the continuous line shows model (C) from Fig. 13 but coming from clouds at $12R_{Schw}$. The spectra were systematically shifted for convenience.

The model specifies the R_X/R_{UV} ratio, but not R_{UV} itself. However, if we assume that the mean quasar spectrum actually corresponds to a mean value of the accretion rate $2.8M_\odot\text{yr}^{-1}$ (i.e. total luminosity 10^{46} erg s^{-1}) and a mean value of the black hole $1.4 \times 10^9 M_\odot$ (after Zheng et al. 1997) the adopted value of the cloud density and the obtained value of the ionization parameter $\xi = 500$ suggest immediately that the representative value of R_{UV} is of order of $12R_{Schw}$. We cannot fully rely on the value of the accretion rate and the mass of the black hole since they depend on the choice of a specific model. However, any reasonable assumption about the luminosity to the Eddington luminosity ratio (of order of 0.1 in this case) would give a similar order of magnitude. Therefore, the kinematic effects are important. In Fig. 15 we show how the soft X-ray emission features are affected by the motion of the clouds. We see that the result is quite sensitive to the actual distances of the clouds from the center. Larger distances, of about $50R_{Schw}$ leave most of the spectral features almost unaffected while considerably smaller values, $7R_{Schw}$, smear out all the features apart from a strong O VIII line which is very broad. Therefore, if soft X-ray

emission is really produced as a reflection spectrum the presence and the strength of the spectral features should help to test the model. Unfortunately, the available data for quasars are not yet of the appropriate quality and there is an additional problem of confusion with the spectral features due to warm absorber.

4.4. Future prospects

The comparison between the theoretical models and the data shown in Sect. 4 did not include spectral fitting in terms of determination of the χ^2 statistics since the cloud model is not ready yet for that kind of quantitative analysis. Clearly, very careful, more advanced computations of both the reflected spectrum and the emission of the dark side of a cloud are necessary in order to decide whether the soft X-ray part of the quasar spectrum can be identified with the radiation reflected by the irradiated sides of the clouds, with some contribution from the primary radiation.

Actually, preliminary computations taking into account multiple scattering (see Paper I) indicate that the amplification is wavelength-dependent as the spectra are steeper in soft X-rays due to this effect. More careful computations based on radiative transfer of soft photons and Monte Carlo computations of X-ray photons show that the slope of the spectrum for $\xi = 300$ has the slope as steep as 2.2 for the reflection component in the 0.2 - 2 keV band due to the multiple reflection (Abrassart et al., in preparation). Such a steep reflection spectrum would allow a primary contribution as high as 0.5 which is only lower by a factor two than expected from a random distribution of the clouds.

The geometrical arrangement of the origin of the primary radiation does not seem equally important as the physical input of the radiative transfer code since the geometrical parameters will adjust themselves to the shapes of the basic spectral components.

Considerable help may be provided by the variability constraints. In the OTCM there are three kinds of variations expected.

The first one is connected with variations of the primary source, or the comptonizing hot medium. Clouds respond to those variations both in optical/UV and in soft X-rays with an average delay of order of the travel time through the region they occupy, $R_{UV} \sim 10R_{Schw}$, of order of some ten thousand of seconds for a $10^8 M_\odot$ black hole.

The second one is connected with a single cloud motion, i.e. the visibility of the primary. These variations are mostly limited to the primary variations and some changes in optical/UV or soft X-rays resulting from the temporary change in geometry are not expected to be delayed in any systematic way. The time-scale of these variations should be of order of the cloud period diminished by the factor describing the relative size of the X-ray source, R_X/R_{UV} , thus not considerably longer than the previous time-scale.

Variations in quasars on those time-scales are unmeasurably weak in the optical band (below 1.2 % in time-scales of hours in 3C 273, von Montigny et al. 1997).

Finally, any systematic changes in the accretion rate in the innermost part of the flow which would both include a change of the level of primary emission as well as of the covering factor should happen on considerably longer time-scales. However, at the present stage the OTCM does not give quantitative predictions of the relative changes of these two factors, although we generally expect that the covering factor should grow with accretion rate, i.e. with bolometric luminosity, thus resulting in harder UV spectra and larger α_{ox} for larger luminosity.

The variability in hard X-ray band for radio quiet quasars also seems to be the best and most direct probe of the nature of the primary source. High quality data for galactic sources allow us to compute the time delays as functions of the Fourier phase as well as the coherence function (e.g. Cui et al. 1997) which strongly support the Comptonization mechanism for the production of 'primary emission' and provide a potentially powerful method to constrain the distribution of the hot gas (e.g. Hua, Kazanas & Titarchuk 1997). The time-scales involved are in the range of 10^{-3} s to 1s for Cyg X-1 so simple minded scaling may suggest time-scales from days to years.

5. Conclusions

Our results suggest that the quasar spectra can be explained within the frame of the optically thick cloud model (OTCM), i.e. as originating in a distribution of irradiated clouds optically thick for electron scattering. One of the important points is that the spectrum in the soft X-ray band is attributed mostly to the reflection from the illuminated partially ionized sides of the clouds. We are not able to definitively distinguish at present if the primary emission comes from the unspecified central source in the form of synchrotron emission or if it originates in the central hot plasma cloud by upscattering of soft photons coming from the clouds. However, we favor the second possibility as the presented results already lead to more self-consistent description for that case.

An alternative picture based on the accretion disk and a corona requires very hot plasma to form the hard X-ray emission and moderately hot but optically thicker plasma to explain the soft X-ray quasar spectra. These two pictures differ with respect to the presence of spectral features since the reflection is accompanied by emission lines and absorption edges which may be used for the purpose of diagnostics. These features are expected to be smeared to some extent by the cloud motion which may help to distinguish them from features arising in a distant warm absorber.

Within the frame of OTCM, the overall shape of the spectrum is very sensitive to the value of the ionization

parameter ξ . Interestingly, the value favored by the comparison of the model to the mean quasar spectrum of Laor et al. (1997) is ~ 500 , in agreement with the energy of the Fe K_α line in moderately bright quasars (Nandra et al. 1997b). Present results allow too low a contribution (by a factor of a few) from the primary emission to account for the observed equivalent width of K_α but we expect that more advanced computations may remove this problem (Abrassart et al., in preparation).

The problem which remains is the prediction of the strong spectral features in the optical/UV band. Observations seem to indicate that no such features are observed in quasar spectra while both OTCM and advanced accretion disk models predict such atomic features although kinematic effects connected with the cloud motion decrease them to some extent. We will address this problem in the future.

Acknowledgements. We are grateful to Suzy Collin for many helpful discussions and detailed comments on the manuscript. We thank Piotr Życki for his help with the high energy reflection code. This work was partially supported by grant 2P03D00410 of the Polish State Committee for Scientific Research and by Jumelage/CNRS No 16 “Astronomie France/Pologne”.

References

- Antonucci R., Barvainis R., 1988, ApJ 332, L13
 Barvainis R., 1993, ApJ 412, 513
 Celotti A., Fabian A.C., Rees M.J., 1992, MNRAS 255, 419
 Collin-Souffrin S., Czerny B., Dumont A.-M., Życki P.T., 1996, A&A 314, 393 (Paper I)
 Cui W., Zhang S.N., Focke W., Swank J.H., 1997, ApJ 484, 383
 Czerny B., Zbyszewska M., 1991, MNRAS 249, 634
 Czerny B., Życki P.T., 1994, ApJL 431, L5
 Done C., Ward M.J., Fabian A.C. et al., 1990, MNRAS, 243, 713
 Edelson R., Alexander D.M., Crenshaw S. et al. 1997, ApJ 470, 364
 Fiore F., Elvis M., Siemiginowska A. et al., 1995, ApJ, 449, 74
 Francis, P.J., Hewett P.C., Foltz C.B. et al. 1991, ApJ 373, 465
 George I., Fabian A.C., 1991, MNRAS, 249, 352
 Gondek D., Zdziarski A.A., Johnson W.N. et al. 1996, MNRAS 282, 646
 Grandi P., Haardt F., Ghisellini G. et al., 1998, ApJ 498, 220
 Guilbert P.W., Rees M.J., 1988, MNRAS 233, 475
 Haardt F., Maraschi L., 1991, ApJL 380, 51
 Hua X.-M., Kazanas D., Titarchuk L., 1997, ApJ 480, L57
 Korista K.T., Alloin D., Morris S.L. et al., 1995, ApJS, 97, 285
 Kuncic Z., Celotti A., Rees M.J., 1997, MNRAS 284, 717
 Laor A., Fiore F., Elvis M., Wilkes B., McDowell J.C., 1997, ApJ 477, 93
 Leach C.M., McHardy I.M., Papadakis I.E., 1995, MNRAS 272, 221
 Lightman A.P., White T.R., 1988, ApJ 335, 57
 Loska Z., Czerny B., 1990, MNRAS 244, 43
 Madejski G.M., Zdziarski A.A., Turner T.J. et al., 1995, ApJ 438, 672
 Maraschi L., Roasio R., Treves A., 1982, ApJ 253, 312
 Mushotzky R.F., Done C., Pounds K.A., 1993, ARA&A 31, 717
 Nandra K., Mushotzky R.F., Yaqoob T., George I.M., Turner T.J., 1997a, MNRAS 284, L7
 Nandra K., George I.M., Mushotzky R.F., Turner T.J., Yaqoob T., 1997b, ApJL 488, L91
 Otani C., Kii T., Reynolds C.S. et al., 1996, PASJ 48, 211
 Pounds K.A., Nandra K., Stewart G.C., George I.M., Fabian A.C., 1990, Nat 344, 132
 Rees M.J., 1987, MNRAS 228, 47
 Ross R.R., Fabian A.C., 1993, MNRAS 261, 74
 Sincell M.W., Krolik J.H., 1997, ApJ 476, 60
 Sivron R., Tsuruta S., 1993, ApJ 402, 420
 Stern B.E., Poutanen J., Svensson R., Sikora M., Begelman M.C., 1995, ApJ 449, 13
 von Montigny C., Aller M., Aller F. et al. 1997, ApJ 483, 161
 Walter R., Fink H.H., 1993, A&A 274, 105
 Williams O.R., et al., 1992, ApJ 389, 157
 Zheng W., Kriss G.A., Telfer R.C., Grimes J.P., Davidsen A.F., 1997, ApJ 475, 469
 Życki P.T., Czerny B., 1994, MNRAS 266, 653